MSW MANAGEMENT -Multidisciplinary, Scientific Work and Management Journal
ISSN: 1053-7899
Vol. 36 Issue 1, 2026, Pages 6611-6616

INFRARED THERMOGRAPHY AND AI TECHNIQUES FOR SOLAR PV HOTSPOT DETECTION: A COMPREHENSIVE ANALYSIS OF ML AND DL FRAMEWORKS

Haresh Dhanji Chande[1]
[1] Research Scholar, Gujarat Technological University, Ahmedabad, Gujarat, India.
Email: hareshchande@gmail.com
Dr. Harikrishna B. Jethva[2]
[2] Associate Professor, Government Engineering College-Gandhinagar, Gujarat Technological University, Gujarat, India.
Jay Prakashbhai Patel[3],
[3] Assistant Professor, Government Engineering College-Patan, Gujarat Technological University, Gujarat, India.
Divyeshkumar Umeshbhai Bavisa[4]
[4] Assistant Professor, Government Engineering College-Patan, Gujarat Technological University, Gujarat, India.

ABSTRACT
The presence of hotspots in solar photovoltaic (PV) panels leads to decreased efficiency of the energy produced, quicker degradation of materials and presents possible safety risks. Hotspots can occur due to shading, defects in the manufacturing process or other fault in the operation of the PV systems. This study proposes a framework based on machine learning for classification of hotspot areas appear in PV modules using thermal imaging and healthy zones in an experimental investigation. The process for identifying those areas is based on automated image patching of thermal images and their consequent classification through various machine learning algorithms: Support Vector Machine (SVM), k-Nearest Neighbours (KNN), Random Forest and Decision Tree models. The success of the models is assessed using explicit measures of effectiveness like accuracy, precision, recall and F1 score. The results obtained from the classification experiments show that the SVM model gave the highest classification efficiency of 94.03% with KNN (91.65%) next, then Random Forest (91.17%) and Decision Tree (83.29%). The results demonstrate that the SVM model gave a higher degree of generalization and robustness than the other classification models for hotspot identification. The proposed algorithm will give a low weight, low computation and non-invasive method of PV fault diagnosis giving improved maintenance procedures and operational reliability of solar energy generation systems. This article also provides an insight into the latest innovations in utilizing machine learning (ML) and deep learning (DL) techniques to identify and locate hotspots found within thermal infrared images.

KEYWORDS: SOLAR PV HOTSPOTS, THERMAL IMAGING, SUPPORT VECTOR MACHINES (SVM), K-NEAREST NEIGHBORS (KNN), RANDOM FOREST (RF), DECISION TREES (DT), FAULT DETECTION.

1. INTRODUCTION
Solar energy is among the important renewable energy sources due to having photovoltaic (PV) panels, which have the capacity for harvesting solar energy. However, the PV panels may exhibit defects such as a hotspot, which may cause damaging features in terms of performance in relation to their efficiency and safety aspects. Recently, the development of thermal and infrared imaging affords a robust way of detecting defects, with the use of machine and deep learning enhancing and automating these systems with respect to their diagnostic capabilities.

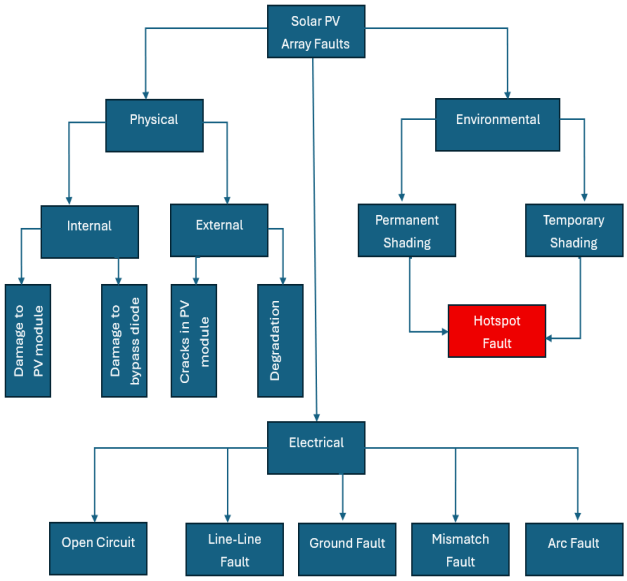

Fig. 1: Classification of Solar PV array faults (Basnet et al., 2020).

As per Figure 1, (Basnet et al., 2020) explored defects in photovoltaic (PV) systems can be basically categorized as physical, environmental and electrical defects, although a different classification system based on the site of installation (systems) or component parts has been discussed. The physical defects are defects found in systems which causes internal and external defects such as microcracking, delamination, solder joint defect or losses due to defects because of aging factors plus environmental installations, due to the installations in the case of soiling, filth, birds droppings or shading of the systems, either on intermittent or temporary basis, due allegedly to some external cause, or on permanent footing, which, as in the past, gives rise to a defective condition, or definite hot spot. The electrical defects are of three kinds, open circuit defects from disconnections, line to line defects from the formation of an undesired, low impedance line created within the array, and then grounding defects, where in a form of leakage in the current, the current is permitted to leak from the otherwise active conductors to the earth. All of these defects are such, as to cause serious loss of energy yield, cause accelerated defects in relation to the parts of the system, and create serious hazards, which relates to modern necessities for testing of defects in a system and eliminates the hazards presented, so as to obtain greater energy yield, and eventually cause less hazard due to the other conditions of accidental defects possible. (He et al., 2023) further emphasized the challenges of compound faults in PV arrays, highlighting the need for multi-label learning to address coupled fault interactions.

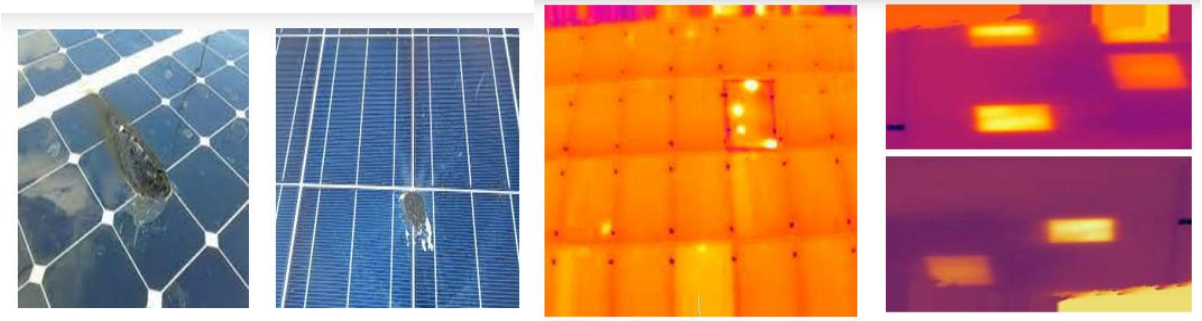

(a) (b) Fig. 2: Solar PV Hotspots: (a) Physical Damage (b) Thermal Image Signature

MSW MANAGEMENT -Multidisciplinary, Scientific Work and Management Journal
ISSN: 1053-7899
Vol. 36 Issue 1, 2026, Pages 6611-6616

The figure 2 summarizes efficiently how hotspots in solar PV are located, demonstrating both their physical manifestation and thermal signature. That is, panel (a) exhibits the physical manifestation of damage, showing the visible damaged and charred areas on solar cell components which are indicative of localised overheating due to shading and defects etc.. Panel (b) shows the thermal image signature where the bright yellow and white areas are indicative of the regions of high temperature or hotspots, which might not be apparent to the naked eye. The figure shows that visual inspection may indicate a more advanced state of physical component degradation, but in temperature thermography identifies the more subtle manifestations of early stages and more internally produced overheating indicative of fault performance.

2. WORK BACKGROUND

2.1. Imaging and Pre-Processing Techniques: Thermography of solar photovoltaic (PV) systems is proceeding with improvement through the use of unmanned aerial vehicles (UAVs). (Akay et al., 2024), for example, carried out thermal UAV inspections in order to prepare orthomosaics from thermal images, discovering temperatures in the color images indicating the presence of hotspots in the solar farms. These hotspots had temperature differences typically in the range of 1 to 8 °C across regions of the solar farms, with no significance for the efficiencies of the solar panels as regards the geographic location. Further, the application of image improvement technology prior to finding faults produces great advantages in thermography inspections of solar installations. For example, (Pathak and Patil, 2023) examined the applications of histogram equalization, contrast limited adaptive histogram equalization (CLAHE), and Gaussian filtering, pointing out that CLAHE increases the contrast of the hotspots by 20-30% and therefore improves the detection capacity in defective solar panels. In particular, image processing technology is used in general thermography for inspection of solar PV installations. (Balachandran et al., 2024) produced a comprehensive review of imaging modalities which help in assessing solar PV installations from IRT and EL imaging to ultraviolet (UV) scanning, as well as image improvement by noise reduction and improved imaging performance, concluding with the development of artificial intelligence (AI) relating to visual faults such as the features of hotspots. (Hong and Pula, 2022) provided an overarching review of PV fault detection methods, underscoring the evolution from traditional to AI-driven classification techniques.

2.2. Traditional Machine Learning Approaches: Conventional means of early fault detection in solar modules called for the ingenuity of feature engineering together with the use of common classifiers. (Ali et al., 2020) proposed a hybrid support vector machine (SVM) framework, which employed red-green-blue (RGB), texture, HOG, and LBP features extracted from IRT images with 96.8% accuracy in training and 92% in testing, in the classification of modules into healthy, non-faulting with hot spots and faulty classes. Correspondingly, (Basnet et al., 2020) presented an intelligent model based on current-voltage (I-V) characteristics and classification using SVM and random forest (RF) algorithms to obtain a means to identify faults, including hot spots. This approach is based on algorithm learning techniques such as random forests which utilises ensemble-type learning (Breiman, 2001), SVM for obtaining an optimal separation margin (Cortes and Vapnik, 1995), k-nearest neighbours (KNN) for pattern recognition (Cover and Hart, 1967) on the basis of spatial properties, decision trees for hierarchical rule-based decision tree formulation (Quinlan, 1986), AdaBoost to add additional weak learners through boosting (Freund and Schapire, 1997) and HOG for the production of gradient oriented features (Dalal and Triggs, 2005). (Chen and Guestrin, 2016) extended ensemble methods with scalable tree boosting (XGBoost), which has shown promise in handling complex PV fault patterns through gradient boosting.

2.3. Advanced Deep Learning Approaches: Deep learning (DL) has major advantages because of the flexibility afforded by its end-to-end extraction and learning competency in hotspot detection tasks. For example, (Pathak et al., 2022) utilized ResNet-50 for hotspot classification, whereby an F1-score of 85.37% was achieved, as well as Faster R-CNN for spatial localization, with mean average precision (mAP) of 67% on IRT images. Unmanned aerial vehicles (UAVs) for autonomous detection, particularly of bird droppings as a leading cause of hotspots, with the implementation of a convolutional encoder-decoder architecture has been provided for by (Moradi Sizkouhi et al., 2021). (Goyal and Rajapakse, 2024) have demonstrated a self-supervised SimSiam architecture for representation learning, which provided an accuracy of 97% for hotspot identification from thermal imagery. (Noura et al., 2025) demonstrated the integration of the DL methodology on EfficientNet and Vision Transformer (ViT) models to provide damage and soiling detection capable of a detection accuracy of 91.8% overall. (Oulefki et al., 2024) utilized unsupervised methodologies based on clustering, augmented with 3D augmented reality (AR) providing better hotspot and snail trail segmentation with Dice scoring of 0.736. Other uses of image registration methodologies have provided fault detection methods of great precision in panoramic views of mountain-top PV plants (Ying et al., 2023), allowing precise mapping not requiring of global positioning system (GPS) data. (Ghahremani et al.,2025) reviewed recent advancements in AI-driven defect detection and localization, emphasizing hybrid DL models for enhanced precision in thermal-based hotspot analysis.

3. METHODOLOGY:

The methodology outlines a pipeline for detecting and classifying hotspots in solar photovoltaic (PV) panels using thermal imagery, leveraging classical machine learning and Evaluation as per shown in Figure 3.

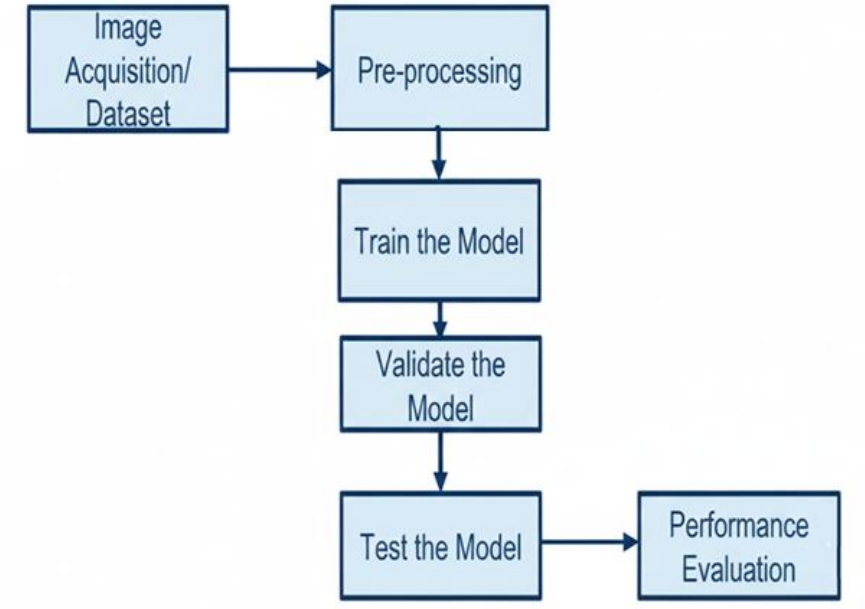

Fig. 3: Methodology (Proposed approach)

3.1. Data Preparation

Dataset Description: The dataset used in this research is called Hotspot Detection in Solar Panel Dataset, which is an open dataset published and maintained by the American University of Sharjah (AUS), and was launched to the public on 16 March, 2023 via the Roboflow Universe web portal. It consists of 1,000 annotated thermal or infrared (IR) images of the photovoltaic (PV) panels, and was produced for object detection purposes which involve identifying the thermal anomalies labelled hotspot and hotspots. Each image has been annotated in order to define those areas of temperature recognition value which have higher recognition values which would indicate the presence of faults in PV modules (American University of Sharjah, 2023). In order that the machine learning experimentation may be properly reproducible and testable, the dataset has been split into three non-overlapping datasets, so that they consist of 722 images for training (72%), 177 images

MSW MANAGEMENT -Multidisciplinary, Scientific Work and Management Journal
ISSN: 1053-7899
Vol. 36 Issue 1, 2026, Pages 6611-6616

for validation (18%) and 101 images for independent testing (10%). This arrangement produces a reliable means of producing testable models, hyper parameter tuning, and a performance measure on objectives which can be repeated in subsequent experimental tests. Thus this dataset is an excellent starting point for the development of automated fault analysis and hotspot detection in solar PV systems, due to its extensive coverage, open access, and accuracy of annotation.

3.1.1. Data Sources: The dataset consists of thermal images of PV panels, each annotated with a polygon defining a hotspot region. The annotations include:

- Polygon coordinates, which are coordinates encircling a hotspot region ($(x_1,y_1),(x_2,y_2)\ldots..(x_4,y_4)$).
- "Healthy" has a binary class label of 0 and "hotspot" has a label of 1.

Thermal images capture temperature variations as grayscale intensity. Polygonal annotations allow for precise localization of hotspots, improving upon bounding box methods. Challenges include the quality of human-generated annotations and variations in image quality.

3.2. Pre-processing:

To make sure the input data used for the detection of the thermal hotspot is consistent and of high quality through a reliable preprocessing pipeline; multiple stages exist within this process including standardizing of the thermal images, reducing noise; all of which contribute an increased performance of the model used to identify hotspots in solar photovoltaic thermal images as described below.

3.2.1 Image Resizing

The first part of the preprocessing process is physically resizing all images to dimensions of 40 x 40 pixels. Resizing the thermal images provides uniformity in the final image dataset to facilitate batch processing and be compatible with the machine learning model used for the final detection of thermal hotspots in photovoltaic images. The additional benefit of resizing is that it creates an efficient means of reducing computing power needed when creating the model, potential memory usage during training, and use of completion time because resizing helps retain sufficient amounts of required spatial information needed to identify hotspots in the thermal images.

3.2.2 Image Grayscale conversion

The second part of the preprocessing process is converting each of the resized thermal images; after being resized, there is now one gray-scale image of thermal data for each pixel out of the original images that contain temperatures. The deduction in the number of color channels when performing the gray-scale conversion is reason for eliminating redundancy and really only keeping information directly related to the identification of thermal hotspots; thus, reducing the amount of computation required by the model when identifying thermal hotspots.

3.2.3 Image Denoising

The third and final part of the preprocessing process is applying a Gaussian filter to each of the thermal images to remove as much of the noise introduced to the thermal images during acquisition (i.e., noise from the sensor, environmental interruptions, etc.) as possible. Thus, enhancing the quality of the resulting filtered image and improving the reliability of all subsequent classification processes for the identification of thermal hotspots in photovoltaic thermal images.

In sum, the overall effect of the preprocessing process is to greatly improve the quality and reduce the variability of the data so that the identification of thermal hotspots in the specific region of interest/ROIs of the photovoltaic thermal images can be detected reliably and accurately.

3.3. Model Training and Evaluation

This section outlines the process of training and evaluating four classifiers on pre-processed image.

3.3.1 Support Vector Machine (SVM): Support Vector Machine (SVM): Support Vector Machine is a supervised algorithm technique that searches for an optimal hyperplane that bisects data points of different classes, finding maximum distance or margin (Cortes & Vapnik, 1995) between these groups. This technique is widely applied to classification as well as regression problems because of its ability to work in high-dimensional space efficiently as per given in eq. 1.

$$\min_{w,b,\xi} \left(\frac{1}{2}\right) ||w||^2 + C \sum_{i=1}^{n} \xi_i \quad (1)$$

Subject to:

$$y_i(w \cdot \phi(x_i) + b) \geq 1 - \xi_i$$

3.3.2 Random Forest: Random Forest is an ensemble or aggregate learning approach, combining a number of decision trees and their responses in order to obtain higher accuracy while controlling over-fitting (Breiman, 2001), applicable both to classification and to regression problems as per shown in eq. 2.

$$Gini = 1 - \sum p_i^2 \quad (2)$$

3.3.3 K-Nearest Neighbors (KNN): K-Nearest Neighbors is a simple algorithmic technique based on non-parametric statistics, and links new data points to those of the majority class among their k-nearest neighbors defined in feature space (Cover & Hart, 1967). The KNN approach is especially successful with small data sets and those with low noise as per eq. 3.

$$d(x, x') = \sqrt{\sum_{i=i}^{n} (x_i - x_i')^2} \quad (3)$$

3.3.4 Decision Tree: Decision Tree techniques recursively subdivide the data into subsets based on the value of the features, so that the resulting hierarchical relationship appears tree-like, thus permitting efficient decision-making (Quinlan, 1986). Decision Tree trees are intuitive, easily interpreted, form the basis for many aggregate methods of which Random Forest is a type.

3.3.5 Evaluation Metrics:

The evaluation metrics of a machine learning method play an important role in measuring the performance of the classification model. The accuracy of the classification model is a measure of the measure of how many of the predicted values were correct including both positive and negative predictions. However, the value of accuracy may be misleading if the dataset is an unbalanced one. When measuring the precision, we would like to see how well the model is likely to predict positive values. The questions involved here are "How many of the instances predicted as positive by the model were indeed correct?" It is useful to analyze, when the costs of false positives are high. Recall is used to measure the ability of the model to find the positive instances. The question relating to recall is "How many of the positive instances were predicted correctly by the model?", it is important when the cost of the false negatives is great. The F1 Score measures the harmonic mean of the Precision and Recall giving a single and balanced measure of the model, and is therefore valuable for the evaluation of models operating on an unbalanced dataset when it is necessary to attempt to achieve a balance between the two. Equations of all mentioned metrices from eq. 4 to 7 are given below:

$$Accuracy = \frac{(TP + TN)}{(TP + TN + FP + FN)} \quad (4)$$

$$Precision = \left(\frac{1}{C}\right) \sum_{i=1}^{C} \left(\frac{TP_i}{(TP_i + FP_i)}\right) \quad (5)$$

$$\text{Recall} = \left(\frac{1}{C}\right) \sum_{i=1}^{C} \left(\frac{TP_i}{(TP_i + FN_i)}\right) \quad (6)$$

$$F1 = \left(\frac{1}{C}\right) \sum_{i=1}^{C} \left(\frac{2 \times Precision_i \times Recall_i}{Precision_i + Recall_i}\right) \quad (7)$$

4. RESULTS AND DISCUSSION

The application of the various types of machine learning models in the detection of solar panel hotspots in the relevant studies present a promising solution. In this respect the parameters which are to the advantages of the relevant work may be said to be the empirical approaches suggested to the actual detection of hotspots. While other approaches are reliable they are extremely exhaustive on the other side and are not all practicable for the large scale PV systems. Introducing thermal and IR imaging other than suggesting empirical approaches, but the models used in this process give a high dividend in automating this field and making it less complicated in the other side rendering it viable.

Table 1 shows the comparative analysis of ML models based on experimental evaluation produce the following performances:

Table 1. Model Performance Metrics

Model	Accuracy	Precision	Recall	F1 Score
SVM	94.03	94.08	90.82	92.27
KNN	91.65	93.46	85.71	88.62
Random Forest	91.17	91.98	85.65	88.13
Decision Tree	83.29	79.19	78.87	79.03

MSW MANAGEMENT -Multidisciplinary, Scientific Work and Management Journal
ISSN: 1053-7899
Vol. 36 Issue 1, 2026, Pages 6611-6616

Among all the models, the Support Vector Machine (SVM) model achieved the best overall performance, with accuracies of 94.03% and precision of 94.08%, sensitivity of 90.82% and F1-score of 92.27%. This performance can be derived from the good generalization that the SVM ensures and also because of the robustness presented in dealing with high dimensionality and of the nonlinearities presented in the input data, which are very likely to be present when the fault detection analysis of images is taken into account. Also, the k-Nearest Neighbors (KNN) classifier presented interesting performances, with an accuracy equals to 91.65%, and precision equals to 93.46%. This means that the learning with respect to the plants relies on a proximity based method, can also be a good learning method, simple and understandable when the amounts of data are moderate, and when there is a good statistics of the local similarity of the input data, it is easier to extract relevant information for logic in the classification.The Random Forest model presented an accuracy equals to 91.17% and showed good stable and consistent results from the point of view of many of them. This is because its proper ensemble procedure for decision making is more robust against noise and variability presented in the input features of the training data, which is corroborated by previous conclusions that the ensemble methods do better in environments of a little more uncertain results.On the other hand, the Decision Tree presented in diameter less results, comparatively, with 83.29% of accuracy and 79.03% of F1-score, suggesting a higher tendency for overfitting and much weaker results regarding generalization. The Decision Tree presented to that respect a good utility in capturing simple decision limits, but the nature of single tree does not allow to have good stability and depth and complexity of analysis to be able to represent correctly the complex processes of thermal formation processes of patterns of vegetation spots.

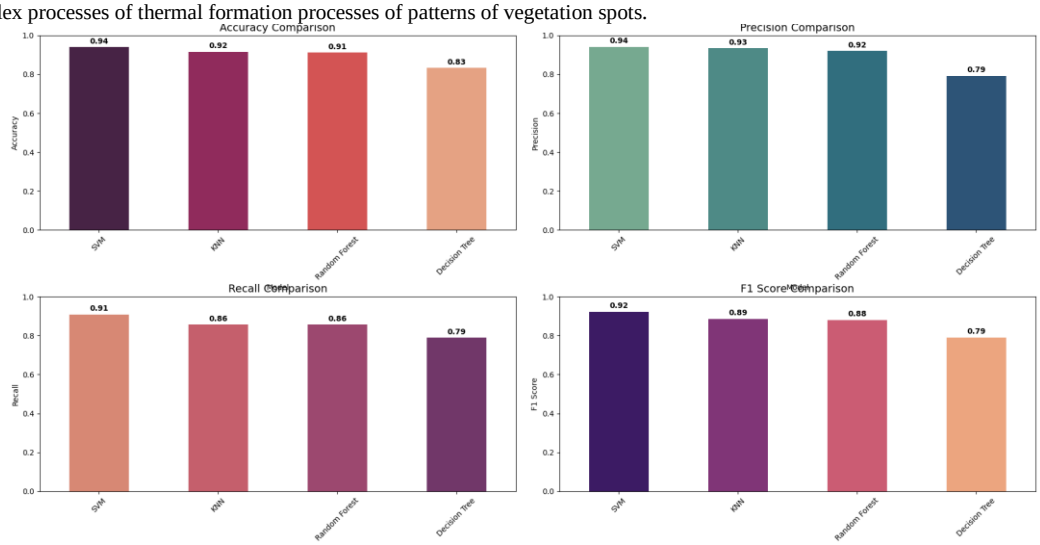

Fig. 6: Bar charts for each metric

The figure 6 Bar charts for each metric presents a performance comparison of the four machine learning classification algorithms Support Vector Machine (SVM), K-nearest Neighbors (KNN), Random Forest and Decision Tree against four important metrics Accuracy, Precision, Recall and F1-Score. The results are shown in four bar charts where SVM is again shown to be the best performing model, achieving the highest scores for the chosen metrics of Accuracy (0.94), Precision (0.94), Recall (0.91) and F1-Score (0.92). KNN and Random Forest give similarly strong performance results, while the Decision Tree algorithm is consistently shown to have relatively low results across the four evaluation metrics (0.83 for Accuracy, 0.79 for Precision, 0.79 for Recall and 0.79 for F1-Score).

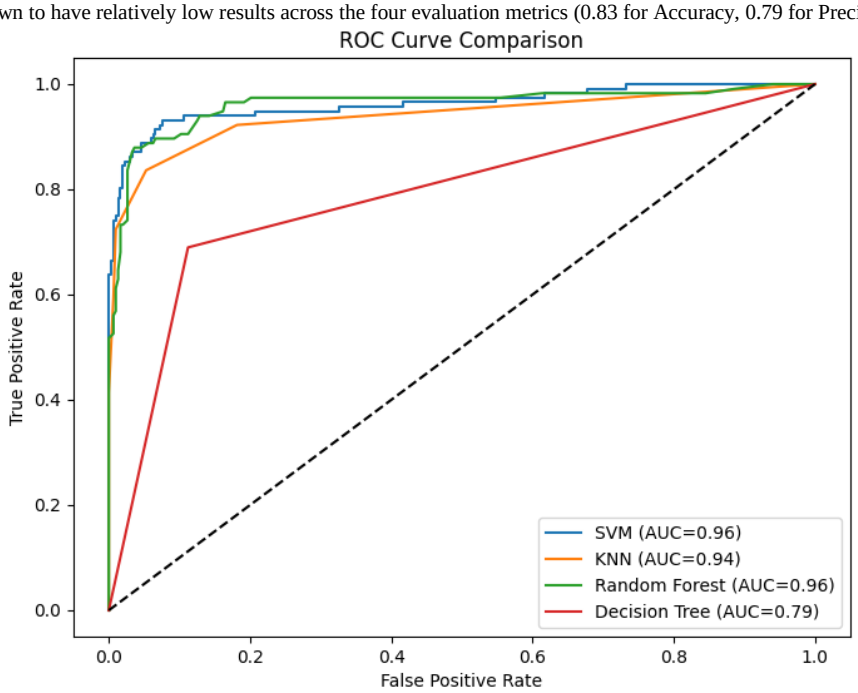

Fig. 7: ROC Curve Comparison of all used ML Models

The figure 7 is the ROC Curve Comparison of four classification models, SVM, KNN, Random Forest and Decision Tree. The ROC (Receiver Operating Characteristic) curve plots the True Positive Rate (Sensitivity) against the False Positive Rate (1 - Specificity) at different thresholds. The figure legend shows the Area Under the Curve (AUC) statistic values indicating the models' ability to discriminate between the two classes, with an AUC value approaching 1.0 interpreting a better performance. The SVM and Random Forest classification models exhibited the best performance in degrees of discriminating ability, with an AUC value of 0.96. This represented a better degree of discriminating power in that the plotted curves approached the upper-left area of the graph. Closely following in performance therefore is given by KNN performance, which is at a slightly lower value with the AUC of 0.94. The worst performance was shown by the Decision Tree algorithm, in that the plotted curve approached the diagonal dashed line (which represents random chance of prediction) and its AUC value of only 0.79.

MSW MANAGEMENT -Multidisciplinary, Scientific Work and Management Journal
ISSN: 1053-7899
Vol. 36 Issue 1, 2026, Pages 6611-6616

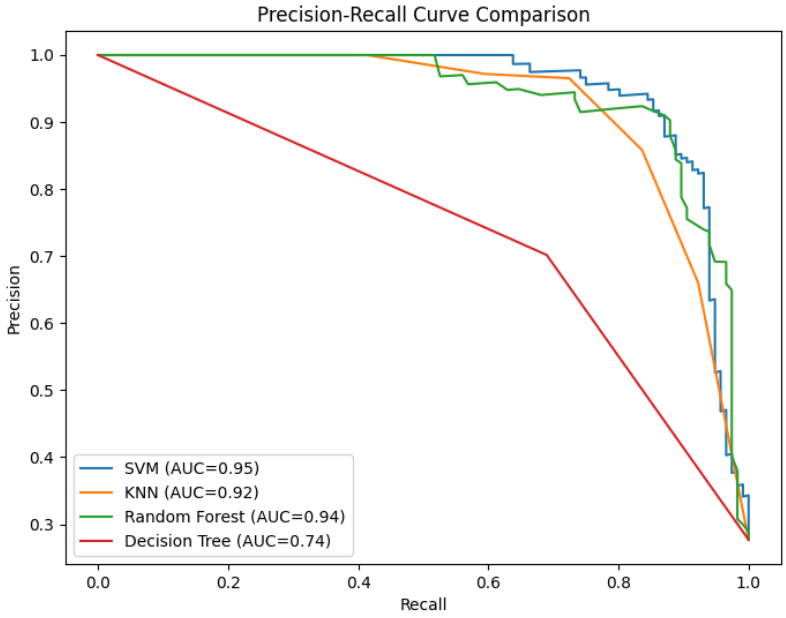

Fig. 8: PR Curve Comparison of all used ML Models

A comparison of various machine learning algorithms in terms of Precision and Recall is presented in the figure 8. This graph shows Precision (The number of positive identifications made and verified positive) on the Y-axis compared to Recall (The number of verified positives) on the X-axis over a varying classification threshold. The area under the curve of the graph (Area Under the Curve = AUC), as stated in the legend, represents a composite indicator of model performance at various thresholds based on Precision and Recall which is desirable to apply in situations where the classifications are imbalanced. The best performing model is the Support Vector Machine (SVM) with (AUC = 0.95) which is in the top right hand corner of the graph. The next best model was the Random Forest implementation which had an AUC = 0.94. The next best algorithm was the K-neighbors Neighbor (KNN) algorithm which had an AUC = 0.92. The algorithm with the poorest performance is the Decision Tree algorithm which has an AUC = 0.74 an indication of very poor performance of this algorithm in regard to the balance between Precision with respect to Recall. The results of this study confirm the results that the proposed pipeline which integrates image pre-processing and SVM Classification produce a user friendly, computationally inexpensive and very accurate result in automated hotspot area detection in PV panels. This type of non-invasive and scalable diagnostic regime could greatly enhance predictive maintenance strategies and the operational reliability of solar photovoltaic systems respectively.

Comparison of Machine Learning and Deep Learning

In comparing both machine learning methods (ML) against modern deep learning methods (DL) for the detection of hot spot(s) in solar modules both represent a trade-off between computational efficiencies versus that of model complexities. On the other hand, even with an continued significant rise in use and popularity of DL since it offers an end-to-end process of feature extraction, classical ML methods will continue to be applicable especially in environments that do not have unlimited resources.

A comparative summary of these technical aspects is presented in Table 2:

Table 2: Comparative Analysis of ML and DL for Thermal Hotspot Detection

Aspect	Machine Learning (ML)	Deep Learning (DL)
Data Requirements	Highly effective with small to moderate datasets (Ali et al., 2020).	Requires massive, diverse datasets for generalization (Goyal and Rajapakse, 2024).
Hardware Resources	**Low:** Executable on standard CPUs and edge devices.	**High:** Requires dedicated GPUs for training/inference (Noura et al., 2025).
Training Latency	Rapid training cycles (minutes to hours).	Extensive training time (hours to days) (Pathak et al., 2022).
Interpretability	**High:** Statistical margins and decision boundaries are clear (Cortes and Vapnik, 1995).	**Low:** Complex internal weights are difficult to interpret (Hong and Pula, 2022).
Deployment	Lightweight; ideal for real-time UAV or IoT monitoring.	Computationally heavy; challenging for edge-side deployment (Akay et al., 2024).

Domain-Specific Suitability for PV Inspection

With respect to Infrared Thermography (IRT), the appropriateness of using either ML or DL is usually a function of the operational deployment. Recent research indicates that DL architecture (i.e. Vision Transformer (ViT), Faster R-CNN) provides very accurate localisations of source hotspots requiring high power & memory to operate (Pathak et al. 2022, Noura et al. 2025). Both Deep learning approaches such as SimSiam achieve hotspot detection accuracy up to 97% (Goyal and Rajapakse 2024) require significant infrastructure, which is typically not available for on-site/who will not be performing the required maintenance while learning.

The findings from this study show that pre-processing with SVM pipeline can achieve 94.03% classification accuracy from the experimental results (Table 1). This indicates that for organized solutions, such as recognizing different types of thermal representations for hotspot identification and limited thermal datasets, classical ML offers an increased opportunity for generating profitable results (Ali et al. 2020, Basnet et al. 2020). Additionally, by including expert-driven features into the models produced using ML, they are able to avoid the "black box" effect of the DL models and give more information about their operation (important for industrial safety reviews and for analyzing how failures occur) (Hong and Pula 2021). ML-based methods show a very high level of robustness when working with structured thermal data at moderate data sample sizes, which fits with real-world PV Inspection scenarios.

While DL is necessary for analyzing unstructured and large datasets, ML has a higher level of interpretability and faster than training, as well as requiring far fewer hardware resources than DL, and therefore serves as the first choice for developing well-tested and reliable PV diagnostic systems that can be used in the field. Further, there is evidence that using hybrid ML-DL frameworks may deliver the greatest benefits from combining the deep feature extractor of DL with the efficient classifier of ML (Ghahremani et al., 2025; Tang et al., 2024).

5. CONCLUSION

Among all the models evaluated, the Support Vector Machine (SVM) model exhibited the best performance metrics, achieving the highest values for accuracy (94.03%), precision (94.08%), recall (90.82%), and F1-score (92.27%). This favorable performance of the SVM classifier is no surprise given its good generalization capabilities and high robustness with respect to high-dimensional data with non-linear data distributions as is commonly found in thermal data. The k-Nearest Neighbors (KNN) model closely followed with respect to performance (accuracy of 91.65%), showing that in case of modest-sized datasets, learning based on proximity can be a very good alternative being both fast and interpretable. The Random Forest model showed to be another good performer with very

MSW MANAGEMENT -Multidisciplinary, Scientific Work and Management Journal
ISSN: 1053-7899
Vol. 36 Issue 1, 2026, Pages 6611-6616

strong and stable performance (accuracy 91.17%), corroborating previous findings that ensemble-based methods generally show good reliability in case of noise and variable input features. On the other hand, the Decision Tree model showed a comparatively poor performance (accuracy 83.29%), indicating a greater tendency towards overfitting and lower generalization capacity when compared with ensemble or margin-based classifiers.

Using preprocessing, the thermal images will be standardized by resizing, converting to grayscale, and completing Gaussian denoising so that all thermal images are the same size, they have no noise, therefore to enhance input image quality and reduce computation complexity will lead to improved accuracy and robustness of the hotspot detection model.

Overall, the results confirm that classical machine learning algorithms can classify hotspots in PV-chains with high performance if effective preprocessing methods are combined, without the computational burden of more advanced models, such as deep learning models. The results suggest that SVM-based models deliver a useful, computationally efficient method of online monitoring of PV health and maintenance systems.

Deep learning models are more accurate than machine learning models, but deep learning models are resource-intensive and can require large amounts of data. Machine Learning models are efficient, flexible, and interpretable so they are often a good choice for applications where you need real-time performance across a variety of scenarios.

Future work could extend these results by incorporating current research in hybrid models that combine the interpretability of classical models with the strength of feature learning in deep learning networks. Further application of spatial–temporal analysis and domain adaptation methods could also increase the generalizability of the framework to different types of PV modules, climatic situations, and imaging environments. (Tang et al., 2024) outline promising techniques for intelligent maintenance in PV plants, including scalable defect diagnosis systems that align with such extensions.

REFERENCES

Basnet, B., Chun, H. and Bang, J. (2020) 'An intelligent fault detection model for fault detection in photovoltaic systems', Journal of Sensors, 2020, pp. 1–11. doi:10.1155/2020/6960328.

He, Z., Chu, P., Li, C. et al. (2023) 'Compound fault diagnosis for photovoltaic arrays based on multi-label learning considering multiple faults coupling', Energy Conversion and Management, 279, 116742. doi:10.1016/j.enconman.2023.116742.

Akay, S.S., Özcan, O. and Yetemen, Ö. (2024) 'Efficiency analysis of solar farms by UAV-based thermal monitoring', Engineering Science and Technology, an International Journal, 53, 101688. doi:10.1016/j.jestch.2024.101688.

Pathak, S.P. and Patil, S.A. (2023) 'Evaluation of effect of pre-processing techniques in solar panel fault detection', IEEE Access, 11, pp. 72848–60. doi:10.1109/ACCESS.2023.3293756.

Balachandran, G.B., Devisridhivyadharshini, M., Ramachandran, M.E. et al. (2024) 'Comparative investigation of imaging techniques, pre-processing and visual fault diagnosis using artificial intelligence models for solar photovoltaic system: A comprehensive review', Measurement, 232, 114683. doi:10.1016/j.measurement.2024.114683.

Hong, Y.-Y. and Pula, R.A. (2022) 'Methods of photovoltaic fault detection and classification: A review', Energy Reports, 8, pp. 5898–929. doi:10.1016/j.egyr.2022.04.043.

Ali, M.U., Khan, H.F., Masud, M. et al. (2020) 'A machine learning framework to identify the hotspot in photovoltaic module using infrared thermography', Solar Energy, 208, pp. 643–51. doi:10.1016/j.solener.2020.08.027.

Breiman, L. (2001) 'Random forests', Machine Learning, 45, pp. 5–32. doi:10.1023/A:1010933404324.

Cortes, C. and Vapnik, V. (1995) 'Support-vector networks', Machine Learning, 20, pp. 273–97. doi:10.1007/BF00994018.

Cover, T. and Hart, P. (1967) 'Nearest neighbor pattern classification', IEEE Transactions on Information Theory, 13(1), pp. 21–7. doi:10.1109/TIT.1967.1053964.

Quinlan, J.R. (1986) 'Induction of decision trees', Machine Learning, 1, pp. 81–106. doi:10.1007/BF00116251.

Freund, Y. and Schapire, R.E. (1997) 'A decision-theoretic generalization of on-line learning and an application to boosting', Journal of Computer and System Sciences, 55, pp. 119–39. doi:10.1006/jcss.1997.1504.

Dalal, N. and Triggs, B. (2005) 'Histograms of oriented gradients for human detection', in Proceedings of the IEEE Computer Society Conference on Computer Vision and Pattern Recognition (CVPR 2005), vol. 1, pp. 886–93. doi:10.1109/CVPR.2005.177.

Chen, T. and Guestrin, C. (2016) 'XGBoost: A scalable tree boosting system', in Proceedings of the 22nd ACM SIGKDD International Conference on Knowledge Discovery and Data Mining, pp. 785–94. doi:10.1145/2939672.2939785.

Pathak, S.P., Patil, S. and Patel, S. (2022) 'Solar panel hotspot localization and fault classification using deep learning approach', Procedia Computer Science, 204, pp. 698–705. doi:10.1016/j.procs.2022.08.084.

Moradi Sizkouhi, A., Aghaei, M. and Esmailifar, S.M. (2021) 'A deep convolutional encoder-decoder architecture for autonomous fault detection of PV plants using multi-copters', Solar Energy, 223, pp. 217–28. doi:10.1016/j.solener.2021.05.029.

Goyal, S. and Rajapakse, J.C. (2024) 'Self-supervised learning for hotspot detection and isolation from thermal images', Expert Systems with Applications, 237, 121566. doi:10.1016/j.eswa.2023.121566.

Noura, H.N., Chahine, K., Bassil, J. et al. (2025) 'Efficient combination of deep learning models for solar panel damage and soiling detection', Measurement, 251, 117185. doi:10.1016/j.measurement.2025.117185.

Oulefki, A., Himeur, Y., Trongtirakul, T. et al. (2024) 'Detection and analysis of deteriorated areas in solar PV modules using unsupervised sensing algorithms and 3D augmented reality', Heliyon, 10, e27973. doi:10.1016/j.heliyon.2024.e27973.

Ying, Y., Ying, P., Men, H. et al. (2023) 'Image registration based fault localization in panoramas of mountain-mounted PV plants', Solar Energy, 256, pp. 16–31. doi:10.1016/j.solener.2023.03.049.

Ghahremani, A., Adams, S.D., Norton, M. et al. (2025) 'Advancements in AI-driven detection and localisation of solar panel defects', Advanced Engineering Informatics, 64, 103104. doi:10.1016/j.aei.2024.103104.

American University of Sharjah (2023) Hotspot detection in solar panel dataset (Version 2) [Dataset]. Roboflow Universe. Available at: https://universe.roboflow.com/american-university-of-sharjah/hotspot-detection-in-solar-panel/dataset/2 (Accessed: 16 March).

Tang, W., Yang, Q., Dai, Z. and Yan, W. (2024) 'Module defect detection and diagnosis for intelligent maintenance of solar photovoltaic plants: Techniques, systems and perspectives', Energy, 297, 131222. doi:10.1016/j.energy.2024.131222.